The Clinically Approved Antifungal Drug Posaconazole Inhibits Human Cytomegalovirus Replication

The Clinically Approved Antifungal Drug Posaconazole Inhibits Human Cytomegalovirus Replication

Beatrice Mercorelli,[a]# Anna Luganini,[b] Marta Celegato,[a] Giorgio Palù,[a] Giorgio Gribaudo,[b] Galina I. Lepesheva,[c] Arianna Loregian [a]#

[a]Department of Molecular Medicine, University of Padua, Padua, Italy

[b]Department of Life Sciences and Systems Biology, University of Turin, Turin, Italy

[c]Department of Biochemistry, Vanderbilt University School of Medicine, Nashville, TN.

Running Head: HCMV Inhibition by Posaconazole

#Address correspondence to Arianna Loregian, arianna.loregian@unipd.it and Beatrice Mercorelli beatrice.mercorelli@unipd.it.

ABSTRACT

Posaconazole (PCZ) is a clinically approved drug used predominantly for prophylaxis and salvage therapy of fungal infections. Here, we report its previously undescribed anti-human cytomegalovirus (HCMV) activity. By antiviral assays we demonstrated that PCZ, along with other azolic antifungals, has a broad anti-HCMV activity being active against different strains including low-passage clinical isolates and strains resistant to viral DNA polymerase inhibitors. Using a pharmacological approach, we identified the inhibition of human cytochrome P450 51 (hCYP51) or lanosterol 14α demethylase, a cellular target of posaconazole in infected cells, as a mechanism of anti-HCMV activity of the drug. Indeed, hCYP51 expression was stimulated upon HCMV infection and the inhibition of its enzymatic activity by either a lanosterol analog (VFV) or PCZ decreased HCMV yield and infectivity of released virus particles. Importantly, we observed that the activity of the first line anti-HCMV drug ganciclovir was tenfold boosted by PCZ and that GCV and PCZ act synergistically in inhibiting HCMV replication. Taken together, these findings suggest that this clinically approved drug deserves further investigation in the development of host-directed antiviral strategies as a candidate anti-HCMV drug with a dual antimicrobial effect.

KEYWORDS: HCMV, antiviral, posaconazole, human CYP51, drug repurposing, synergism.

Human cytomegalovirus (HCMV) is a ubiquitous beta-herpesvirus that infects from 60% to nearly 80% of the human population worldwide and establishes a life-long persistence in the host characterized by sporadic reactivations in healthy individuals (1). HCMV is also a major opportunistic human pathogen, which causes life-threatening diseases in subjects with acquired or developmental immunodeficiency, such as transplant recipients or immune naïve fetuses. Indeed, HCMV causes deafness and neurological disorders in approximately 0.1% of congenital infections (2). Moreover, HCMV has been suggested as a cofactor of vascular diseases and immune senescence (3).

To date, to prevent and treat HCMV infections, there is no vaccine available, and only a limited number of drugs are licensed for treatment: ganciclovir (GCV), its oral prodrug valganciclovir, foscarnet, acyclovir, its prodrug valacyclovir, cidofovir, and the recently approved letermovir (4,5). Currently, all the available anti-HCMV drugs target virus-encoded proteins, i.e., the DNA polymerase and the terminase (5). The clinical use of these antivirals can have several drawbacks, such as an unfavorable safety profile characterized by severe acute or long-term toxicity and poor oral bioavailability (4). Moreover, no drug has been approved for the treatment of congenital infection (6) and the management of HCMV infections can be further complicated by the emergence of drug-resistant HCMV strains (7,8). For all these reasons, there is still a strong need to develop new, safe, and effective antiviral compounds, possibly endowed with a new mechanism of action.

HCMV, like many other viruses, hijacks several cellular pathways and deeply alters many host physiological processes in order to replicate efficiently (9). Thus, the development of host-directed antiviral strategies could be an alternative or an additional approach to treat HCMV-associated diseases (10), as well as to overcome viral resistance issues. In this

regard, drug repurposing can represent a powerful strategy for the identification of host pathways and factors playing a role during viral replication (11-13). Based on this rationale, we followed this strategy to identify new compounds and targets for anti-HCMV intervention through a drug screening and follow-up studies that identified several novel HCMV inhibitors, including both approved drugs and natural compounds (12,14,15).

Here, we report the discovery of the previously undescribed anti-HCMV activity of posaconazole (PCZ), a drug approved for the prophylaxis and salvage therapy of systemic fungal infections. Our study stems from the observation that drugs belonging to the class of azolic antifungals were identified in two previous independent drug repurposing screenings for inhibitors of HCMV replication (12,16,17). Starting from this observation, we initially evaluated the antiviral activity of a panel of azolic antifungals used both topically and for the treatment of invasive fungal infections. PCZ, which was not present in our original screened library, showed an interesting anti-HCMV activity, thus we decided to characterize further its antiviral mechanism. In the recent years, the antiviral properties of azolic antifungals has been an emerging topic and PCZ, together with itraconazole, was found to have activity against both positive-stranded RNA viruses, such as picornaviruses and flaviviruses (11,18,19), and against negative-stranded RNA viruses, such as Ebola virus and influenza virus (20,21).

We investigated deeper the anti-HCMV activity of PCZ and found that its antiviral activity was related to its inhibitory activity against human cytochrome P450 51 (hCYP51, or lanosterol 14α demethylase). This enzyme is the most conserved cytochrome P450, as well as the only that catalyzes demethylation of lanosterol (22), being involved in both cholesterogenesis and synthesis of essential regulatory sterols during meiosis (23). Fungal

CYP51 is the target of PCZ and other antifungals in the treatment of mycosis, however our study suggests that human CYP51 is involved in the antiviral mechanism of PCZ against HCMV.

Noteworthy, our data indicate that a combination of PCZ with GCV, the gold standard for anti-HCMV therapy, greatly potentiates the antiviral effect of the latter and is synergistic in inhibiting HCMV replication in infected cells. Thus, this study provides the rationale for a possible clinical validation of the anti-HCMV activity of PCZ alone or in combination with GCV.

RESULTS

Anti-human cytomegalovirus activity of approved azolic antifungals. In a drug repurposing campaign, we previously identified a series of molecules endowed with anti-HCMV activity, among which we noticed an overrepresentation of drugs belonging to the class of azolic antifungals (12). To extend this knowledge, a more complete panel of azolic antifungal drugs was analyzed for anti-HCMV activity (Table 1). As shown in Fig. 1A, in plaque reduction assays (PRA), posaconazole (PCZ) and ketoconazole (KTZ) showed a dose-dependent inhibitory effect on HCMV AD169 replication in HFF cells, similarly to what we previously reported for clotrimazole, econazole, and miconazole (12). On the other hand, under the same experimental conditions, fluconazole (FCZ), voriconazole (VCZ), and itraconazole (ITZ) did not exhibit significant anti-HCMV activity (Fig. 1B).

Then, to exclude the possibility that the antiviral activity of PCZ might be due to cytotoxicity, its effect on the viability of uninfected HFFs cells was evaluated by MTT

assays. As reported in Table 1, we found that the antiviral activity of posaconazole was not due to cytotoxicity of the target cells, since a significant toxic effect was not observed at concentrations up to 250 μM.

Broad anti-HCMV activity of posaconazole and other antifungals. To investigate the spectrum of anti-HCMV activity of PCZ and of other antifungals, we repeated the antiviral assays with a panel of HCMV strains, including three different low passage-number clinical isolates (TB40-UL32-EGFP, VR1814, and 388438U). As reported in Figure 2, the anti-HCMV activity of PCZ was not dependent on the viral strain, since the EC_{50} values obtained with different HCMV strains were comparable (Table 2). Next, we evaluated the activity of PCZ against HCMV strains resistant to the available viral DNA polymerase inhibitors, as the emergence of drug resistance is an increasing cause of transplant failure associated with HCMV infections, in particular after prolonged antiviral therapy (24). PCZ fully inhibited the replication of viruses with mutations in *UL54* gene conferring cross-resistance to GCV and cidofovir or to foscarnet and acyclovir (strains 759^{r}D100 and PFA^{r}D100, respectively, Table 2). Anti-HCMV activity against different strains was found also for MCZ and ECZ (Table 2), two other antifungal drugs emerged for anti-HCMV activity during the drug repurposing screening (12).

Finally, the inhibitory activity of PCZ against HCMV resulted not cell type-dependent, since the EC_{50} values measured for the TR strain in epithelial (EC_{50} = 4.2 μM) and endothelial (EC_{50} = 4.8 μM) cells were in line to that observed in fibroblasts (EC_{50} = 3.7 μM) (Table 2). Moreover, since TR strain is naturally resistant to GCV and CDV, we obtained further evidence of the activity of PCZ against HCMV clinical strains resistant to DNA polymerase inhibitors.

Taken together these results indicated that PCZ and other antifungals could have a mechanism of action different from that of anti-HCMV drugs targeting the viral DNA polymerase.

Effects of PCZ treatment on HCMV yield. PCZ is routinely used as a systemic drug to prevent and treat fungal infections in immunosuppressed patients (25), thus, we decided to focus on this molecule, given that a potential dual antifungal and antiviral effect could be relevant in this clinical setting. To better characterize the anti-HCMV activity of PCZ, we also evaluated its effects on the production of virus progeny in a multi-cycle viral growth experiment. PCZ reduced the production of HCMV infectious progeny in a dose-dependent manner as revealed by virus yield reduction assays (Table 3). In sum, we observed that treatment of HCMV-infected cells with PCZ after infection resulted in the inhibition of viral replication and progeny production.

Inhibition of human CYP51, a host target of posaconazole, correlates with anti-HCMV activity. PCZ is known to interfere with different host pathways (26-29), among which there are cholesterol homeostasis and synthesis mediated by human CYP51, the rate-limiting enzyme in late-stage cholesterogenesis (28-30). Thus, we exploited VFV, the most potent enzymatic inhibitor of hCYP51 identified so far (30), to investigate the involvement of hCYP51 during HCMV replication. Like other azolic compounds, VFV inhibits human CYP51 by binding in the enzyme active site and competing with the substrate lanosterol. In enzymatic assays *in vitro*, both VFV and PCZ inhibited the initial rate of lanosterol conversion catalyzed by purified hCYP51 with IC_{50} values of 0.5 and 8 µM, respectively (Fig. 3A and Table 3). This was not observed with VCZ (IC_{50} >100 µM), which served as a negative control in the enzymatic assays (Fig. 3A and Table 3). When tested by PRA, VFV

caused a dose-dependent inhibitory effect on HCMV replication (Fig. 3B), albeit with an EC_{50} value higher than that of PCZ (13.3 µM *versus* 3.3 µM). However, given the highly hydrophobic nature of VFV (LogP 5.4), we reasoned that VFV could be poorly soluble in the semi-solid medium used for PRAs, thus virus yield reduction assays with VFV were also performed. VFV showed indeed a strong and dose-dependent inhibitory effect on infectious virus production with an EC_{50} in the low-micromolar range (Fig. 3C and Table 3), thus suggesting that hCYP51 enzymatic activity is required for the production of infectious HCMV progeny.

HCMV infection activates hCYP51 expression. Since we observed that hCYP51 enzymatic activity is required for HCMV replication, next we investigated whether its expression could be modulated during viral infection. Indeed, under normal conditions (i.e., cells grown in regular cholesterol-containing medium), the cholesterol biosynthetic pathway is not stimulated. To analyze the modulation of *hCYP51* promoter upon HCMV infection, we transfected permissive U-373 MG cells with a plasmid encoding a reporter gene under the control of *hCYP51* promoter and then infected them with HCMV. As shown in Fig. 4A, infection with HCMV activated *hCYP51* promoter by about 40-fold. This upregulation was not observed when the transfected cells were infected with a UV-inactivated virus, which is able to bind and enter into the cells but not to express viral genes, arguing that *de novo* synthesized HCMV proteins are required for *hCYP51* promoter activation (Fig. 4A). Upon infection of serum-fed HFFs, a ~2-fold increase in *hCYP51* mRNA level was observed during the early phase of HCMV replication (Fig. 4B) and an accumulation of hCYP51 protein throughout the virus cycle was accordingly detected by both Western blot (Fig. 4C

and Fig. S1) and immunofluorescence analysis in living cells (Fig. S2). Altogether, these data support the view that HCMV infection activates *hCYP51* gene expression.

Inhibition of hCYP51 enzyme during HCMV replication reduces the infectivity of viral progeny. As shown above, both VFV and PCZ inhibited hCYP51 enzyme, which catalyzes the rate-limiting step in late cholesterogenesis. Thus, treatment of HCMV-infected cells with these inhibitors should reduce *de novo* cholesterol synthesis during HCMV replication. The intracellular presence of cholesterol during HCMV infection and within the virus particle has been related to the infectivity of HCMV virions (31). We therefore hypothesized that the virus particles produced in cells treated with hCYP51 inhibitors might be less infective. To test this, we determined the particle-to-PFU ratio of cell-free HCMV released from infected HFF cells treated with PCZ, VFV, or DMSO as a control, assuming that each virus particle (infectious or defective) contained one genome. Treatment of HCMV-infected cells for 120 h with either PCZ or VFV significantly reduced both the number of HCMV genomes (Fig. 5A) and the infectivity of viral progeny, with a ~7-10-fold increase in particle-to-PFU ratio with respect to DMSO-treated infected cells (Fig. 5B). Altogether, the results from this section indicated that hCYP51 enzymatic activity is required in the context of productive HCMV replication and could contribute to the generation of infectious HCMV particles.

GCV and PCZ act synergistically against HCMV replication in infected cells. We also tested by PRAs the antiviral efficacy of GCV in the absence or the presence of a dose of PCZ (3 μM) approximately equivalent to the mean concentration found in plasma by therapeutic drug monitoring of patients treated with PCZ (25). Noteworthy, in the presence of PCZ, GCV was ~10-fold more potent against HCMV than in the presence of the vehicle

DMSO (EC_{50} 0.13 µM for the combination of GCV + PCZ *versus* 1.44 µM for GCV + DMSO, Fig. 6). Considering these results, we investigated further the effects of the combination of PCZ with GCV against the replication of HCMV AD169 by PRAs. As reported in Table 4, the combination of GCV and PCZ resulted in antiviral synergism at all drug combinations tested, since the Combination Index (CI) values calculated by applying the Chou & Talalay method (32) resulted all <0.9 (Table 4). We did not observe any evident cell cytotoxicity when the drugs were tested in combination, thus the synergistic effect on the reduction of viral plaques number was most likely the result of combining two drugs with different targets and mechanisms of action. Beside a reduction in the absolute number, we also observed a clear reduction in the size of the plaques when GCV was used in combination with PCZ. The calculated Dose Reduction Indexes are reported in Table S3. Although future trials will be required to validate this observation in a clinical setting, these results suggest that a combination of GCV and PCZ might represent a new therapeutic strategy for the management of HCMV infections.

DISCUSSION

Our study stems from the observation of an overrepresentation of drugs belonging to the class of azolic antifungals among the molecules selected in a previous drug repurposing screening aimed at identifying new anti-HCMV compounds (12). Starting from this observation, we report for the first time that posaconazole, a drug already approved and used in both adult and pediatric immunosuppressed patients for prevention and as salvage therapy of fungal infections, is a potent inhibitor of HCMV replication in the low micromolar range.

By characterizing the anti-HCMV profile of PCZ, we found that upon treatment of infected cells with PCZ and VFV, two inhibitors of hCYP51 enzyme, the infectivity of the released HCMV particles is significantly reduced. Azolic antifungals have shown a polypharmacological profile mainly by affecting host cholesterol homeostasis and trafficking (26-29), in addition to be active against several unrelated viruses (11,18-21). In human cells, PCZ is known to interfere with several pathways, such as cholesterol trafficking from lysosomes by inhibiting the Niemann-Pick C1 protein transporter (26) and from ER by inhibiting oxysterol-binding protein (OSBP) cholesterol-shuttling protein (11,19), as well as cholesterogenesis by inhibiting hCYP51 enzyme (29,30). The inhibition of OSBP, the target of PCZ against single-stranded positive RNA viruses, might be however likely excluded as a possible mechanism of anti-HCMV activity of PCZ on the basis of the anti-HCMV activity exhibited also by imidazolic antifungals such as miconazole and econazole (Table 1 and Table 2), which do not bind OSBP (12,19).

The reduced infectivity of HCMV particles released from PCZ-treated cells could be caused by the block of cholesterol trafficking and hCYP51 inhibition caused by the drug, leading to lower levels of available cholesterol. In fact, changes in the cholesterol uptake and efflux have been observed during HCMV infection (31,33), and it has been reported that virion cholesterol content is crucial for the infectivity of HCMV progeny (31). Later during infection, when appropriate levels of new cholesterol molecules could be required by HCMV to produce infectious virions, inhibition of hCYP51-mediated cholesterogenesis exerted by PCZ would thus have a detrimental effect on the infectivity of the released viral progeny. However, this hypothesis remains to be tested. Nonetheless, our data suggest a role of the late cholesterogenesis mediated by hCYP51 in the production of infectious HCMV virions.

253 Indeed, we found that HCMV induces hCYP51 expression during infection. Importantly, a
254 functional role for hCYP51 in the context of productive HCMV infection was validated by a
255 pharmacological approach with the enzymatic inhibitors VFV and PCZ. Furthermore, the
256 observed decrease in virus yield and in infectivity of virus particles produced upon inhibition
257 of hCYP51 enzymatic activity supports the view that new cholesterol molecules are indeed
258 required for the generation of infectious virus particles. Accumulation of new cholesterol
259 molecules might contribute in conferring appropriate membrane fluidity to the enlarged
260 cytomegalic cell, in the organization of virion, or in the targeting and proper localization of
261 viral proteins within the envelope or mature virus particle. Accordingly, in other virus
262 models, both virion cholesterol content and effective cholesterogenesis have been reported to
263 affect virus infectivity. Depletion of cholesterol during hepatitis B virus infection was shown
264 to induce in fact a topologic change of the large envelope protein that renders the virus non-
265 infectious (34). Interestingly, also HIV-1 Nef protein induces hCYP51 expression to increase
266 *de novo* cholesterol synthesis and enhance virions infectivity (35), and low levels of
267 cholesterogenesis and cholesterol uptake have been related to a lower HIV trans-infection
268 ability and a slower disease progression *in vivo* (36).

269 Posaconazole peak levels (Cmax) in plasma of treated patients either under
270 prophylaxis or treatment of invasive fungal infections depend on a series of different factors,
271 among which there are the formulation, the posology, the diet, and of course the
272 administered dose (37). During prophylaxis in patients at high risk of both fungal and
273 HCMV infections and for therapeutic use in the treatment of mycosis, posaconazole peak
274 levels are reported to be averagely 1.5-2 µg/ml, corresponding to 2.2-2.9 µM (41-42), and
275 thus approximately equal to or below the EC_{50}s that we found for posaconazole against

276 HCMV (Table 2). However, anti-HCMV activity for posaconazole within a clinically
277 achievable range could be obtained either by synergistic combination with GCV or by
278 developing a better formulation.

279 We also observed that PCZ exerted anti-HCMV activity against both wild-type
280 clinical isolates and drug-resistant viral strains in a cell-type independent manner.
281 Importantly, we demonstrated that GCV and PCZ act synergistically in inhibiting HCMV
282 replication in infected cells with a combination effect ranging from moderate to very strong
283 synergism. The analysis of our data with Calcusyn software allowed the determination of the
284 simulated Dose Reduction Index (DRI) for both GCV and PCZ. DRI estimates the extent to
285 which GCV levels may be reduced when used in synergistic combination with PCZ to
286 achieve effect levels compared with GCV used alone (32). For example, 90% inhibition of
287 HCMV replication may be potentially obtained by reducing by 10- and 6-fold GCV and
288 PCZ, respectively (Table S3), a condition that could be clinically achievable in treated
289 patients. However, this simulation remains to be clinically tested *in vivo*.

290 In conclusion, our study suggests that repurposing of posaconazole against HCMV
291 both alone and in combination with GCV could foster the development of new antiviral
292 strategies against this important viral pathogen, exploiting its dual antimicrobial activity, and
293 contribute to understand how HCMV manipulates host pathways for a productive replication.
294
295
296 **MATERIALS AND METHODS**

297 **Compounds.** Ganciclovir (GCV), foscarnet (FOS), and all the antifungal drugs were
298 from Sigma-Aldrich. Cidofovir (CDV, Vistide) was from Gilead Sciences. VFV ((*R*)-*N*-(1-

(3,4'-difluoro-[1,1'-biphenyl]-4-yl)-2-(1*H*-imidazol-1-yl)ethyl)-4-(5-phenyl-1,3,4-oxadiazol-2-yl)benzamide) was synthesized at Vanderbilt University as described (43). For cellular assays, 100× stock of VFV was prepared in 25% dimethylsulfoxide (DMSO)/34% aqueous 2-hydroxypropyl-β-cyclodextrin (v/v) purchased from Sigma.

Cells and viruses. Human Foreskin Fibroblast (HFF), ARPE-19, and U-373 MG were all from the American Type Culture Collection (ATCC) and were cultured in Dulbecco modified Eagle's medium (DMEM) (Life Technologies) supplemented with 10% fetal bovine serum (FBS, Life Technologies), 100 U/ml penicillin, and 100 µg/ml streptomycin sulfate (P/S, both from Life Technologies). Human dermal microvascular endothelial cells (HMVECs) (CC-2543) were obtained from Clonetics and cultured in endothelial growth medium (EGM) (Clonetics). All cell cultures were maintained at 37°C in a humidified atmosphere supplemented with 5% CO_2.

HCMV (strain AD169) was purchased from the ATCC. HCMV TB40E-UL32-EGFP (kindly provided by C. Sinzger, University of Ulm, Germany) was previously described (44) as well as HCMV VR1814 (kindly provided by G. Gerna, IRCCS Policlinico San Matteo, Pavia, Italy) recovered from a cervical swab from a pregnant woman (45). HCMV 388438U clinical isolate was collected from a urine sample at the Microbiology and Virology Unity of Padua University Hospital (Italy) and was under passage 4 after primary isolation. HCMV strains resistant to antiviral drugs were obtained from the NIH AIDS Research and Reference Reagent Program (Rockville, MD) and previously described (46). HCMV TR was reconstituted by transfecting HFFs with the corresponding TR-BAC that was prepared from the TR clinical strain resistant to GCV and CDV and isolated from an ocular specimen (47).

Reconstitution of BAC-derived TR strain in fibroblasts generated infectious virus that retaines the ability to infect both endothelial and epithelial cells (48).

Plaque reduction assays. Plaque reduction assays (PRAs) with HCMV were performed as previously described (49). Briefly, HFF, ARPE-19, and HMVEC cells were seeded at a density of 1.5×10^5 cells per well in 24-well plates. The next day, the cells were infected at 37°C with 80 Plaque Forming Unit (PFU) per well of the different viruses in serum-free DMEM. At 2 h p.i., the inocula were removed, cells were washed, and media containing various concentrations of each compound, 2% FBS, and 0.6% methylcellulose were added. After 10 days of incubation at 37°C, cell monolayers were fixed and stained with crystal violet, and viral plaques were counted.

Cytotoxicity assays. The cytotoxicity of tested compounds was determined by the 3-(4,5-dimethylthiazol-2-yl)-2,5-diphenyl tetrazolium bromide (MTT; Sigma-Aldrich) method as described previously (50).

Virus yield reduction assays. For virus yield reduction assays, HFF cells were plated at 2×10^4 cells per well in 96-well plates, incubated overnight, and infected the next day with HCMV AD169 at MOI = 0.1 PFU/cell. After virus adsorption for 2 h at 37°C, cells were washed and incubated with 0.2 ml of fresh medium containing 5% FBS in the absence or in the presence of test compounds. Plates were incubated for 5 days at 37°C, and then subjected to one cycle of freezing and thawing. Titres were determined by transferring 0.1 ml aliquots from each well to a fresh 96-well monolayer culture of HFF cells, followed by 1:5 serial dilutions across the plate. Cultures were incubated for 7 days and at the end of incubation they were fixed and stained, and the numbers of plaques were determined.

343 **Enzymatic assays *in vitro*.** Recombinant human CYP51 and its redox partner
344 NADPH-cytochrome P450 reductase (CPR) were expressed in *Escherichia coli* and purified
345 as described previously (30). The standard reaction mixture contained 0.5 µM hCYP51 and
346 1.0 µM CPR), 100 µM L-*α*-1,2-dilauroyl-*sn*glycerophosphocholine, 0.4 mg/ml isocitrate
347 dehydrogenase, and 25 mM sodium isocitrate in 50 mM potassium phosphate buffer (pH 7.2)
348 containing 10% glycerol (v/v). After addition of the radiolabeled ([3-^{3}H]) lanosterol (~4,000
349 dpm/nmol; dissolved in 45% HPCD, w/v, final concentration 50 µM) and inhibitors
350 (concentration range 0.1 - 20 µM), the mixture was preincubated for 30 s at 37 °C in a
351 shaking water bath, the reaction was initiated by the addition of 100 µM NADPH and
352 stopped by extraction of the sterols with 5 ml of ethyl acetate. The extracted sterols were
353 dried, dissolved in methanol, and analyzed by a reversed-phase HPLC system (Waters)
354 equipped with a *β*-RAM detector (INUS Systems) using a NovaPak octadecylsilane (C_{18})
355 column and a linear gradient water/acetonitrile/methanol (1.0:4.5:4.5, v/v/v) (solvent A) to
356 CH_3OH (solvent B), increasing from 0 to 100% B for 30 min at a flow rate of 1.0 ml/min.
357 The IC_{50} values were calculated using GraphPad Prism 6, with the percentage of lanosterol
358 converted being plotted against inhibitor concentration and the curves fitted with non-linear
359 regression (log(inhibitor) vs. normalized response - variable slope).

360 **Plasmids.** The pCYP51-luc plasmid, which contains the −314/+343 human *CYP51*
361 (*hCYP51*) gene promoter region upstream of the luciferase reporter gene was kindly
362 provided by D. Rozman (Centre for Functional Genomics and Bio-Chips Institute of
363 Biochemistry, Faculty of Medicine University of Ljubljana, Slovenia) and was previously
364 described (51). pGAPDH-eGFP plasmid, which contains the promoter region of cellular

365 *GAPDH* gene upstream of the *enhanced Green Fluorescent Protein* (eGFP) gene was
366 previously described (41) and used as a control of transfection efficiency.

367 **Cell transfections and HCMV infection.** For the transfection/infection experiments
368 with HCMV, U-373 MG cells were grown on 24-well plates and co-transfected using
369 calcium phosphate (Calcium Phosphate Transfection Kit, Sigma) with 1 µg of pCYP51-luc
370 plasmid along with 0.2 µg of pGAPDH-eGFP plasmid as a control to normalize transfection
371 efficiency. The next day, transfected cells were either mock-infected or infected with HCMV
372 AD169 at MOI = 0.5 PFU/cell for 2 h and then incubated with 5% FBS-containing medium.
373 At 48 h post-infection, luciferase activity as well as eGFP expression were measured. For all
374 the experiments, the values were normalized by dividing the values obtained for luciferase
375 (LU) by the fluorescence units (FU) obtained for eGFP expression and expressed as relative
376 luciferase units (RLU). For UV-inactivation, a procedure previously described was followed
377 (52). Briefly, HCMV diluted in serum-free DMEM was exposed for 8 min at a distance of 4
378 cm under a UV-light (VL-6MC, 254 nM, 6w). Inactivation of the virus was assessed by
379 immunofluorescence.

380 **Quantification of gene expression.** HFF cells were seeded in 6-well plates at 6×10^5
381 cells/well and incubated o/n at 37°C. In case of infection, the next day they were infected
382 with HCMV AD169 at MOI = 1 PFU/cell for 2 h and then incubated with 5% FBS-
383 containing medium. Total RNA was extracted from samples collected at different times p.i.
384 using a total RNA Purification Plus Kit (Norgen Biotek) according to the manufacturer's
385 protocol. cDNA was generated from RNA (2 µg) using random primers (Applied
386 Biosystems) and M-MLV reverse transcriptase (Applied Biosystems). qPCR was performed
387 with SYBR green reagent (Applied Biosystems) according to the manufacturer's instructions

on a 7900 HT Fast Real-Time PCR System (Applied Biosystems) using primers for *hCYP51*, *GAPDH*, and HCMV *UL54* genes (sequences reported in Table S1). The relative changes in gene expression were calculated by means of the ΔΔCt method (53) using *GAPDH* to normalize data.

Western Blot. For the analysis by Western blot of the induction hCYP51 during HCMV infection, subconfluent HFF cells in 6-well plates were infected with HCMV AD169 at a MOI = 0.5 PFU/cell. Whole-cell protein extracts were prepared at different times as previously described (12) and then analyzed by Western blot with different antibodies listed in Table S2. Immunocomplexes were detected with the appropriate secondary anti-immunoglobulin Abs conjugated to horseradish peroxidase (Life Technologies). Densitometry analysis was performed with ImageJ software (https://imagej.nih.gov/ij/).

Immunofluorescence and confocal microscopy analysis. For confocal laser-scanning microscopy analysis, HFFs were infected with HCMV AD169 at an MOI = 0.25 PFU/cell. At different times p.i., cells were fixed with 4% paraformaldehyde in PBS 1× for 15 min at room temperature and then permeabilized with 0.1% Triton X-100 in PBS for 20 min at RT. After washing extensively with PBS, cells were incubated first with 4% FBS in PBS for 1 h at room temperature and then with different primary antibodies (listed in Table S2) diluted in FBS 4% in PBS 1× for 1 h at 37°C under shaking. Cells were then washed extensively with 4% FBS in PBS 1× and incubated with secondary fluorochrome-conjugated antibodies (listed in Table S2) for 1 h at 37 °C. Nuclei were stained by incubation for 20 min with Draq5 (1:8,000 in PBS 1×). Cells were imaged using a Nikon Eclipse Ti-E microscope.

Particle-to-PFU ratio determination. To determine the particle-to-PFU ratio of HCMV produced in the presence of test compounds, HFFs were seeded at 2×10^4 cells per

411 well in 96-well plates, incubated overnight, and infected the next day with HCMV AD169 at
412 MOI = 0.5 PFU/cell. After virus adsorption for 2 h at 37°C, cells were washed and incubated
413 with 0.2 ml of fresh medium containing 5% FBS in the presence or in the absence of test
414 compounds. Plates were incubated for 5 days at 37°C. At the end of the incubation, 0.05 ml
415 of supernatants were used to determine the number of virus particles that were produced
416 under the different experimental conditions, while 0.05 ml were titrated on fresh monolayers
417 of HFF cells as previously described, to determine the number of PFUs present in the same
418 volume of supernatant. For virus particles determination, 0.05 ml of supernatants were
419 incubated with 0.2% SDS and proteinase K for 1 h at 56°C and then for 15 min at 95°C to
420 inactivate proteinase K. Then, viral DNA was extracted with DNA purification kit (Promega)
421 and quantified by qPCR as described below. The particle-to-PFU ratio was determined by
422 dividing the number of HCMV genomes by the number of PFU determined in the same
423 volume of supernatant derived from the same sample.

424 **Quantification of viral genomes.** To quantify the HCMV genomes in 0.05 ml of
425 supernatants derived from the different samples collected at 120 h p.i., quantitative Real-
426 Time PCR (qPCR) was performed as previously described (46). The number of viral
427 genomes was normalized to the cellular *β-globin* gene copies. The sequences of the
428 oligonucleotides used are listed in Table S1.

429 **Drug combination studies.** To evaluate the combined effects of PCZ and GCV on
430 HCMV AD169 replication, plaque reduction assays were performed as described above
431 using 0.25x, 0.50x, 1x, 2x, and 4x EC_{50} for each combination of PCZ and GCV at equipotent
432 ratio. The 2-drug combination effects were assessed using the Chou-Talalay method (32)

based on mass-action law based dynamic theory computed in the CalcuSyn software version 2.0 (Biosoft, Cambridge, UK).

Statistical analysis. All statistical analyses were performed using GraphPad Prism version 6.0.

SUPPLEMENTAL MATERIAL

Supplemental material to this article may be found at journal website.

ACKNOWLEDGMENTS

This work was supported by University of Padua (STARS Consolidator Grant FINDER to B.M.); by Associazione Italiana per la Ricerca sul Cancro (AIRC, grant n. IG18855 to A. Loregian); by Ministero dell'Istruzione, dell'Università e della Ricerca, Italy (PRIN 2017 n. 2017KM79NN to A. Loregian, and PRIN 2017 n. 2017HWPZZZ to A. Luganini); by British Society for Antimicrobial Chemotherapy, UK (grant BSAC-2018-0064 to A. Loregian); by University of Turin (Local Research Funds to G.G. and A.Luganini); by Fondazione Umberto Veronesi (to M.C.); and by a grant from the National Institutes of Health, USA (GM067871) to G.I.L.. The funders had no role in study design, data collection and interpretation, or the decision to submit the work for publication. We thank D. Rozman, G. Pari, and M. Mach for providing plasmids; C. Sinzger and G. Gerna for providing some of the viruses used in this study, and L. Messa and T. Hargrove for experimental assistance.

DECLARATION OF INTERESTS

B.M., A. Luganini, G.G., and A. Loregian have filed a provisional patent on the use of posaconazole alone and in combination with ganciclovir for the treatment of pathological condition(s) associated with cytomegalovirus infection.

REFERENCES

1. Griffiths P, Baraniak I, Reeves M. 2015. The pathogenesis of human cytomegalovirus. J Pathol 235:288-297.
2. Britt WJ. 2018. Maternal immunity and the natural history of congenital human cytomegalovirus infection. Viruses 10: E405.
3. Klenerman P, Oxenius A. 2016. T cell responses to cytomegalovirus. Nat Rev Immunol 16:367-377.

4. Mercorelli B, Sinigalia E, Loregian A, Palù G. 2008. Human cytomegalovirus DNA replication: antiviral targets and drugs. Rev Med Virol 18:177-210.
5. Britt WJ, Prichard MN. 2018. New therapies for human cytomegalovirus infections. Antiv Res 159:153-174.
6. Manicklal S, Emery VC, Lazzarotto T, Boppana SB, Gupta RK. 2013. The "silent" global burden of congenital cytomegalovirus. Clin Microbiol Rev 26:86-102.
7. Meesing A, Razonable RR. 2018. New developments in the management of cytomegalovirus infection after transplantation. Drugs 78:1085-1103.
8. Douglas CM, Barnard R, Holder D, Leavitt R, Levitan D, Maguire M, Nickle D, Teal V, Wan H, van Alewijk DCJG, van Doorn LJ, Chou S, Strizki J. 2019. Letermovir Resistance Analysis in a Clinical Trial of Cytomegalovirus Prophylaxis for Hematopoietic Stem Cell Transplant Recipients. J Infect Dis pii: jiz577.
9. Shenk T, Alwine JC. 2014. Human cytomegalovirus: coordinating cellular stress, signaling, and metabolic pathways. Ann Rev Virol 1:355-374.
10. Munger J, Bennett BD, Parikh A, Feng X-J, McArdle J, Rabitz HA, Shenk T, Rabinowitz JD. 2008. Systems-level metabolic flux profiling identifies fatty acid synthesis as a target for antiviral therapy. Nat Biotechnol 26:1179-1186.
11. Strating JRPM, van der Linden L, Albulescu L, Bigay J, Arita M, Delang L, Leyssen P, van der Schaar HM, Lanke KH, Thibaut HJ, Ulferts R, Drin G, Schlinck N, Wubbolts RW, Sever N, Head SA, Liu JO, Beachy PA, De Matteis MA, Shair MD, Olkkonen VM, Neyts J, van Kuppeveld FJ. 2015. Itraconazole inhibits enterovirus replication by targeting the oxysterol-binding protein. Cell Rep 10:600-615.
12. Mercorelli B, Luganini A, Nannetti G, Tabarrini O, Palù G, Gribaudo G, Loregian A. 2016. Drug Repurposing Approach Identifies Inhibitors of the Prototypic Viral Transcription Factor IE2 that Block Human Cytomegalovirus Replication. Cell Chem Biol 23:340-351.
13. Mercorelli B, Palù G, Loregian A. 2018. Drug Repurposing for Viral Infectious Diseases: How Far Are We? Trends Microbiol 26:865-876.
14. Mercorelli B, Luganini A, Celegato M, Palù G, Gribaudo G, Loregian A. 2018. Repurposing the clinically approved calcium antagonist manidipine dihydrochloride as a new early inhibitor of human cytomegalovirus targeting the Immediate-Early 2 (IE2) protein. Antiv Res 150:130-136.
15. Luganini A, Mercorelli B, Messa L, Palù G, Gribaudo G, Loregian A. 2019. The isoquinoline alkaloid berberine inhibits human cytomegalovirus replication by interfering with the viral Immediate Early-2 (IE2) protein transactivating activity. Antiviral Res 164:52-60.
16. Nukui M, O'Connor CM, Murphy EA. 2018. The Natural Flavonoid Compound Deguelin Inhibits HCMV Lytic Replication within Fibroblasts. Viruses 10:pii: E614.
17. Mercorelli B, Luganini A, Palù G, Gribaudo G, Loregian A. 2019. Drug Repurposing Campaigns for Human Cytomegalovirus Identify a Natural Compound Targeting the Immediate-Early 2 (IE2) Protein: A Comment on "The Natural Flavonoid Compound Deguelin Inhibits HCMV Lytic Replication within Fibroblasts". Viruses 11:pii: E117.
18. Rhoden E, Nix, Weldon WC, Selvarangan R. 2018. Antifungal azoles itraconazole and posaconazole exhibit potent in vitro antiviral activity against clinical isolates of parechovirus A3 (Picornaviridae). Antiviral Res 149:75-77.

19. Meutiawati F, Bezemer B, Strating JRPM, Overheul GJ, Žusinaite E, van Kuppeveld FJM, van Cleef KWR, van Rij RP. 2018. Posaconazole inhibits dengue virus replication by targeting oxysterol-binding protein. Antiviral Res 157:68-79.
20. Sun W, He S, Martínez-Romero C, Kouznetsova J, Tawa G, Xu M, Shinn P, Fisher E, Long Y, Motabar O, Yang S, Sanderson PE, Williamson PR, García-Sastre A, Qiu X, Zheng W. 2017. Synergistic drug combination effectively blocks Ebola virus infection. Antiviral Res 137:165-172.
21. Schloer S, Goretzko J, Kühnl A, Brunotte L, Ludwig S, Rescher U. 2019. The clinically licensed antifungal drug itraconazole inhibits influenza virus in vitro and in vivo. Emerg Microbes Infect 8:80-93.
22. Lepesheva GI, Waterman MR. 2007. Sterol 14alpha-demethylase cytochrome P450 (CYP51), a P450 in all biological kingdoms. Biochim Biophys Acta 1770:467-477.
23. Debeljak N, Fink M, Rozman D. 2003. Many facets of mammalian lanosterol 14alpha-demethylase from the evolutionarily conserved cytochrome P450 family CYP51. Arch Biochem Biophys 409:159-171.
24. Razonable RR. 2018. Drug-resistant cytomegalovirus: clinical implications of specific mutations. Curr Opin Organ Transplant 23:388-394.
25. Clark NM, Grim SA, Lynch JP, 3rd. 2015. Posaconazole: use in the prophylaxis and treatment of fungal infections. Sem Resp Critical Care Med 36:767-785.
26. Trinh MN, Lu F, Li X, Das A, Liang Q, De Brabander JK, Brown MS, Goldstein JL. 2017. Triazoles inhibit cholesterol export from lysosomes by binding to NPC1. Proc Natl Acad Sci USA 114:89-94.
27. Chen B, Trang V, Lee A, Williams NS, Wilson AN, Epstein EH Jr, Tang JY, Kim J. 2016. Posaconazole, a second-generation triazole antifungal drug, inhibits the Hedgehog signaling pathway and progression of basal cell carcinoma. Mol Cancer Ther 15:866-876.
28. Lamb DC, Kelly DE, Waterman MR, Stromstedt M, Rozman D, Kelly SL. 1999. Characteristics of the heterologously expressed human lanosterol 14alpha-demethylase (other names: P45014DM, CYP51, P45051) and inhibition of the purified human and Candida albicans CYP51 with azole antifungal agents. Yeast 15:755-763.
29. Strushkevich N, Usanov SA, Park H-W. 2010. Structural basis of human CYP51 inhibition by antifungal azoles. J Mol Biol 397:1067-1078.
30. Hargrove TY, Friggeri L, Wawrzak Z, Sivakumaran S, Yazlovitskaya EM, Hiebert SW, Guengerich FP, Waterman MR, Lepesheva GI. 2016. Human sterol 14alpha-demethylase as a target for anticancer chemotherapy: towards structure-aided drug design. J Lipid Res 57:1552-1563.
31. Gudleski-O'Regan N, Greco TM, Cristea IM, Shenk T. 2012. Increased expression of LDL receptor-related protein 1 during human cytomegalovirus infection reduces virion cholesterol and infectivity. Cell Host Microbe 12:86-96.
32. Chou TC. 2006. Theoretical basis, experimental design, and computerized simulation of synergism and antagonism in drug combination studies. Pharmacol Rev 58: 621–681.
33. Low H, Mukhamedova N, Cui HL, McSharry BP, Avdic S, Hoang A, Ditiatkovski M, Liu Y, Fu Y, Meikle PJ, Blomberg M, Polyzos KA, Miller WE, Religa P, Bukrinsky M, Soderberg-Naucler C, Slobedman B, Sviridov D. 2016.

Cytomegalovirus restructures lipid rafts via a US28/CDC42-mediated pathway, enhancing cholesterol efflux from host cells. Cell Rep 16:186-200.

34. Dorobantu C, Macovei A, Lazar C, Dwek RA, Zitzmann N, Branza-Nichita N. 2011. Cholesterol depletion of hepatoma cells impairs hepatitis B virus envelopment by altering the topology of the large envelope protein. J Virol 85:13373-13383.

35. Zheng Y-H, Plemenitas A, Fielding CJ, Peterlin BM. 2003. Nef increases the synthesis of and transports cholesterol to lipid rafts and HIV-1 progeny virions. Proc Natl Acad Sci USA 100:8460-8465.

36. Rappocciolo G, Jais M, Piazza P, Reinhart TA, Berendam SJ, Garcia-Exposito L, Gupta P, Rinaldo CR. 2014. Alterations in cholesterol metabolism restrict HIV-1 trans infection in nonprogressors. mBio 5:e01031-13.

37. Dekkers BGJ, Bakker M, van der Elst KCM, Sturkenboom MGG, Veringa A, Span LFR, Alffenaar JC. 2016. Therapeutic Drug Monitoring of Posaconazole: an Update. Curr Fungal Infect Rep 10:51-61.

38. Kersemaekers WM, Dogterom P, Xu J, Marcantonio EE, de Greef R, Waskin H, van Iersel ML. 2015. Pharmacokinetics and safety study of posaconazole intravenous solution administered peripherally to healthy subjects. Antimicrob Agents Chemother 59:1246-1251.

39. Krishna G, Moton A, Ma L, Medlock MM, McLeod J. 2009. Pharmacokinetics and absorption of posaconazole oral suspension under various gastric conditions in healthy volunteers. Antimicrob Agents Chemother 53:958-966.

40. Leelawattanachai P, Montakantikul P, Nosoongnoen W, Chayakulkeeree M. 2019. Pharmacokinetic/pharmacodynamic study of posaconazole delayed-release tablet in a patient with coexisting invasive aspergillosis and mucormycosis. Ther Clin Risk Manag 15:589-595.

41. Cornely OA, Duarte RF, Haider S, Chandrasekar P, Helfgott D, Jiménez JL, Candoni A, Raad I, Laverdiere M, Langston A, Kartsonis N, Van Iersel M, Connelly N, Waskin H. 2016. Phase 3 pharmacokinetics and safety study of a posaconazole tablet formulation in patients at risk for invasive fungal disease. J Antimicrob Chemother 71:718-726.

42. Cornely OA, Robertson MN, Haider S, Grigg A, Geddes M, Aoun M, Heinz WJ, Raad I, Schanz U, Meyer RG, Hammond SP, Mullane KM, Ostermann H, Ullmann AJ, Zimmerli S, Van Iersel MLPS, Hepler DA, Waskin H, Kartsonis NA, Maertens J. 2017. Pharmacokinetics and safety results from the Phase 3 randomized, open-label, study of intravenous posaconazole in patients at risk of invasive fungal disease. J Antimicrob Chemother 72:3406-3413.

43. Lepesheva G, Christov P, Sulikowski GA, Kim K. 2017. A convergent, scalable and stereoselective synthesis of azole CYP51 inhibitors. Tetrahedron Lett 58:4248-4250.

44. Sampaio KL, Cavignac Y, Stierhof YD, Sinzger C. 2005. Human cytomegalovirus labeled with green fluorescent protein for live analysis of intracellular particle movements. J Virol 79:2754-2767.

45. Revello MG, Lilleri D, Zavattoni M, Stronati M, Bollani L, Middeldorp JM, Gerna G. 2001. Human cytomegalovirus immediate-early messenger RNA in blood of pregnant women with primary infection and of congenitally infected newborns. J Infect Dis 184:1078-1081.

46. Mercorelli B, Muratore G, Sinigalia E, Tabarrini O, Biasolo MA, Cecchetti V, Palù G, Loregian A. 2009. A 6-aminoquinolone compound, WC5, with potent and selective anti-human cytomegalovirus activity. Antimicrob Agents Chemother 53:312-315.
47. Murphy E, Yu D, Grimwood J, Schmutz J, Dickson M, Jarvis MA, Hahn G, Nelson JA, Myers RM, Shenk T. 2003. Coding potential of laboratory and clinical strains of human cytomegalovirus. Proc Natl Acad Sci USA 100:14976–14981.
48. Cavaletto N, Luganini A, Gribaudo G. 2015. Inactivation of the Human cytomegalovirus US20 gene hampers productive viral replication in endothelial cells. J Virol 89:11092–11106.
49. Loregian A, Mercorelli B, Muratore G, Sinigalia E, Pagni S, Massari S, Gribaudo G, Gatto B, Palumbo M, Tabarrini O, Cecchetti V, Palù G. 2010. The 6-aminoquinolone WC5 inhibits human cytomegalovirus replication at an early stage by interfering with the transactivating activity of viral immediate-early 2 protein. Antimicrob Agents Chemother 2010; 54:1930-40.
50. Loregian A, Coen DM. 2006. Selective anti-cytomegalovirus compounds discovered by screening for inhibitors of subunit interactions of the viral polymerase. Chem Biol 13:191-200.
51. Halder SK, Fink M, Waterman MR, Rozman D. 2002. A cAMP-responsive element binding site is essential for sterol regulation of the human lanosterol 14alpha-demethylase gene (CYP51). Mol Endocrinol 16:1853-1863.
52. Chaumorcel M, Lussignol M, Mouna L, Cavignac Y, Fahie K, Cotte-Laffitte J, Geballe A, Brune W, Beau I, Codogno P, Esclatine A. 2012. The human cytomegalovirus protein TRS1 inhibits autophagy via its interaction with Beclin 1. J Virol 86:2571-2584.
53. Livak KJ, Schmittgen TD. 2001. Analysis of relative gene expression data using real-time quantitative PCR and the 2(-Delta Delta C(T)) Method. Methods 25:402-408.

FIGURE LEGENDS

FIG 1 Susceptibility of HCMV to approved azolic antifungals. Plaque reduction assays were performed in HFF infected with HCMV and treated with different doses (from 0.1 to 25 µM) of the indicated test compounds or GCV as a control. (A) Dose-dependent inhibition of HCMV AD169 replication by PCZ and KTZ. (B) Absence of significant inhibition of HCMV AD169 replication by FCZ, ITZ, and VCZ. (ITZ could be tested only up to 10 µM due to solubility issues). Graph represents mean ± SD of n ≥ 3 independent experiments in duplicate.

642 **FIG 2 Dose-dependent inhibition of the replication of indicated HCMV strains by**
643 **posaconazole.** Plaque reduction assays were performed in HFF infected with the indicated
644 HCMV strains and treated with different doses (from 0.1 to 25 μM) of PCZ. Graphs
645 represents mean ± SD of n = 3 independent experiments in duplicate.
646 **FIG 3 Inhibition of host hCYP51 affects HCMV replication.** (A) Inhibition of enzymatic
647 activity of purified hCYP51 by VFV, PCZ, and VCZ (2 min reaction). Graph represents the
648 mean ± SD of n = 3 independent experiments in duplicate. (B) Plaque reduction assays were
649 performed in HFF infected with HCMV AD169 and treated with different doses (from 0.1 to
650 25 μM) of hCYP51 inhibitor VFV. Graphs represent the mean ± SD of n ≥ 3 independent
651 experiments in duplicate. (C) Dose-dependent inhibition by VFV of virus progeny
652 production in HCMV-infected HFFs as determined by virus yield reduction assays. Graph
653 represents the mean ± SD of n = 4 independent experiments in duplicate.
654 **FIG 4 hCYP51 expression is activated during HCMV infection.** (A) Activation of
655 *hCYP51* promoter in U-373 MG cells mock-infected or infected with either HCMV AD169
656 or UV-inactivated HCMV. Reported data are expressed as Relative Luciferase Units
657 (LU/FU, RLU), which are the luciferase units normalized to the fluorescence units derived
658 from the expression of the co-transfected *eGFP* reporter gene. Graph represents the mean ±
659 SD of n = 3 independent experiments in duplicate. Data were analyzed by a one-way
660 ANOVA followed by Tukey's multiple comparison tests. ***p≤0.0001; ****p<0.0001. (B)
661 Analysis of *hCYP51* mRNA levels upon HCMV infection of HFF cells determined by qPCR
662 at the indicated times. The mRNA levels of *UL54* were detected as a control for the
663 progression of the infection at 24 and 48 h p.i. mRNA levels were normalized to cellular
664 *GAPDH* and gene expression was reported as relative quantification (RQ) compared to

665 calibrator sample (mock-infected cells for *hCYP51* and HCMV-infected cells at 24 h p.i. for
666 *UL54*). Graph represents the mean ± SD of n = 3 independent experiments in duplicate. (C)
667 Analysis of hCYP51 and viral proteins expression during HCMV replication. Host hCYP51
668 protein and viral IE antigens (IEA) were detected by Western blot both in mock-infected
669 HFFs (M) and in HFFs infected with HCMV at an MOI = 0.5 PFU/cell at the indicated h p.i.
670 Detection of host β-actin was used as a loading control. Molecular weights in kDalton are
671 indicated on the left. Image of a representative experiment is showed.

672 **FIG 5 Effects of hCYP51 enzymatic activity inhibition on HCMV replication and**
673 **infectivity.** (A) Pharmacological inhibition of hCYP51 reduces the number of HCMV
674 genomes. HFF cells infected with HCMV at MOI = 0.5 PFU/cell were treated with 10 μM
675 PCZ or VFV, or 0.1% DMSO as a control for 120 h. HCMV genome copies in the
676 supernatant of each sample were then determined by qPCR. Graph represents the mean ± SD
677 of n = 3 independent experiments in quadruplicate. Data were analyzed by a one-way
678 ANOVA followed by Dunnett's multiple comparison test. ***p<0.001; **p<0.005 compared
679 to control (DMSO-treated, infected sample). (B) Pharmacological inhibition of hCYP51
680 reduces the infectivity of viral particles. Particle-to-PFU ratios were obtained by dividing the
681 number of HCMV particles collected from supernatants derived from HFFs infected at MOI
682 = 0.5 PFU/cell and treated with test compounds (determined by qPCR) by the viral titers
683 obtained in the same sample volume (determined by titration on fresh monolayers). Graph
684 represents the mean ± SD of n = 3 independent experiments in quadruplicate. Data were
685 analyzed by a one-way ANOVA followed by Dunnett's multiple comparison tests. *p<0.05;
686 **p<0.005, compared to control (DMSO-treated, infected sample).

687 **FIG 6 Therapeutic dose of posaconazole enhances anti-HCMV activity of ganciclovir.**
688 Antiviral efficacy of GCV against HCMV AD169 in the absence (+ DMSO) or the presence
689 (+ PCZ) of 3 μM PCZ as determined by PRA. Graph represents the mean ± SD of n ≥ 3
690 independent experiments in duplicate.
691
692
693
694
695
696

Table 1. Antiviral activity of antifungal drugs against HCMV AD169

Compound (Abbreviation)	EC_{50}[b] (µM)	CC_{50}[c] (µM)	SI[d]
Clotrimazole (CTZ)[a]	0.8 ± 0.6	40 ± 28	50
Econazole (ECZ)[a]	5.7 ± 1.7	85 ± 13	17
Fluconazole (FCZ)	> 25	>250	>10
Itraconazole (ITZ)	>10	N.D.	N.D.
Ketoconazole (KTZ)	14.4 ± 4.6	116 ± 6	8
Miconazole (MCZ)[a]	3.2 ± 0.8	55 ± 16	17
Posaconazole (PCZ)	3.3 ± 0.5	>250	>76
Voriconazole (VCZ)	> 25	> 250	>10
Ganciclovir (GCV)	2.3 ± 0.6	>500	>217

[a] Reported in Reference 12.
[b] 50% Effective Concentration, the compound concentration that inhibits 50% of plaque formation, as determined by PRAs against HCMV AD169 in HFF cells. Reported values represent the means ± SD of data derived from n ≥ 3 independent experiments in duplicate. GCV was included as a positive control.
[c] Compound concentration that produces 50% of cytotoxicity, as determined by MTT assays in HFF cells. Reported values represent the means ± SD of data derived from two independent experiments in duplicate.
[d] SI, Selectivity Index (determined as the ratio between CC_{50} and EC_{50}).
N.D., Not Determined.

Table 2. Antiviral activity of antifungal drugs against different HCMV strains in different cell types

HCMV strain	Cell type	Antiviral activity EC_{50}[a] (µM)			
		ECZ	MCZ	PCZ	Control[b]
TB40-UL32-EGFP	HFF	4.5 ± 0.7	3.8 ± 0.4	3.5 ± 1.8	3.5 ± 0.7
VR1814	HFF	3.9 ± 2.1	4.3 ± 1.1	3.5 ± 0.7	2.3 ± 1.3
388438U	HFF	N.D.	N.D.	3.2 ± 0.4	3.2 ± 0.8
759^{r}D100	HFF	4.3 ± 1.1	4.5 ± 1.8	2.6 ± 1.2	75 ± 12
GDG^{r}P53	HFF	3.4 ± 0.9	2.6 ± 0.3	3.5 ± 1.1	1.9 ± 1.8
PFA^{r}D100	HFF	4.2 ± 0.1	3.7 ± 0.6	4.8 ± 1.5	250 ± 18
TR	HFF	N.D.	N.D.	3.7 ± 1.3	N.D.
TR	ARPE-19	N.D.	N.D.	4.2 ± 1.8	N.D.
TR	HMVEC	N.D.	N.D.	4.8 ± 2.0	N.D.

[a] 50% Effective Concentration, the compound concentration that inhibits 50% of plaque formation, as determined by PRAs in HFFs, and for TR strain also in epithelial (ARPE-19) and endothelial (HMVECs) cells. Reported values represent the means ± SD of data derived from n ≥ 3 independent experiments in duplicate.
[b] GCV was used as a control for all strains except for PFA^{r}D100, for which FOS was used.
N.D., Not Determined.

Table 3. Activity of posaconazole and VFV in virus yield reduction assays and in enzymatic assays *in vitro*

Compound	Antiviral Activity (µM)		Inhibitory Activity (µM)
	EC_{50}[a]	EC_{90}[b]	IC_{50}[c]
PCZ	2.2 ± 1.1	7.1 ± 1.1	8.0 ± 2.5
VFV	1.2 ± 0.9	10.1 ± 1.3	0.5 ± 0.2
VCZ	N.D.	N.D.	>100

[a] 50% Effective Concentration, the compound concentration that inhibits 50% of virus yield, as determined by titration in HFF cells. Reported values represent the means ± SD of data derived from n = 4 independent experiments in duplicate.

[b] 90% Effective Concentration, the compound concentration that inhibits 90% of virus yield, as determined by titration in HFF cells. Reported values represent the means ± SD of data derived from n = 4 independent experiments in duplicate.

[c] 50% Inhibitory Concentration, the compound concentration that causes a 50% decrease in the rate of lanosterol conversion, as determined by reconstitution of the hCYP51 activity *in vitro*, 2 min reaction. Reported values represent the means ± SD of data derived from n = 3 independent experiments in duplicate and calculated using GraphPad Prism 6.0 (dose-response –inhibition).

N.D., Not Determined.

Table 4. Analysis of the effects of the combination of GCV and PCZ against HCMV replication

GCV/PCZ combination at equipotent ratio (fold of EC_{50}[a])	CI[b]	Drug Combination effect[c]
0.25	0.625 ± 0.169	Synergism
0.5	0.780 ± 0.031	Moderate synergism
1	0.353 ± 0.278	Synergism
2	0.075 ± 0.039	Very strong synergism
4	0.064 ± 0.042	Very strong synergism

[a] Fold of 50% Effective Concentration for GCV/PCZ yielding an equipotent concentration ratio between the two combined drugs. The EC_{50} values was determined by PRAs against HCMV AD169 in HFF cells for each drug alone or in combination at concentrations starting from 4-fold to 0.25-fold the equipotent ratio of the drugs considering ratio 1:1.33, approximated values from Table 1.

[b] Combination Index, obtained by computational analysis with Calcusyn software. Reported values represent means ± SD of data derived from n = 3 independent experiments in triplicate.

[c] Drug combination effect defined as: very strong synergism for CI<0.1; strong synergism for 0.1<CI<0.3; synergism for 0.3<CI<0.7; moderate synergism for 0.7<CI<0.9, according to (32).

814 **Figure 1**

815

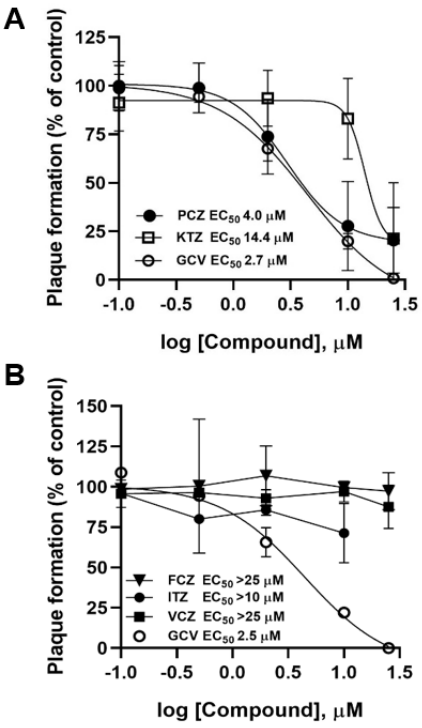

816

817

818

819

820

821

822

823

824

825 **Figure 2**

826

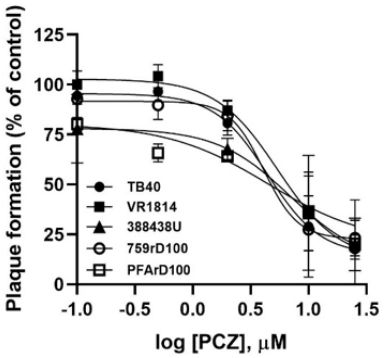

827

828

829

830

831

832

833

834

835

836

837

838

839

840

841

842

843 **Figure 3**

844

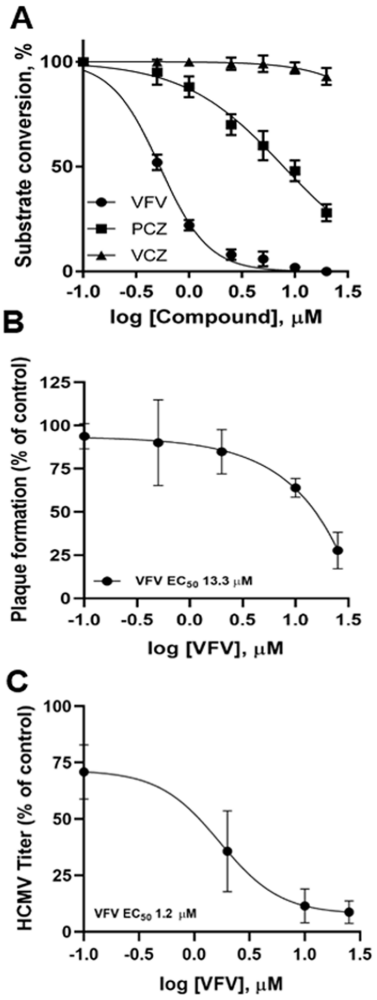

845

846

847

848

849

Figure 4

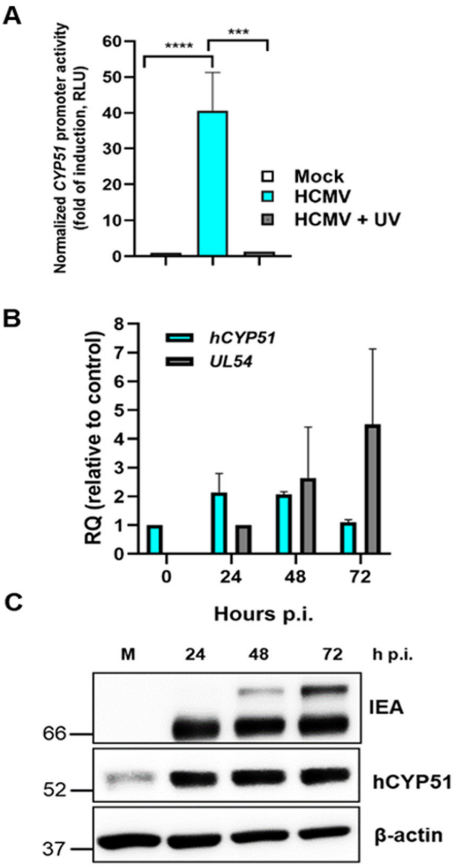

860

861 **Figure 5**

862

863

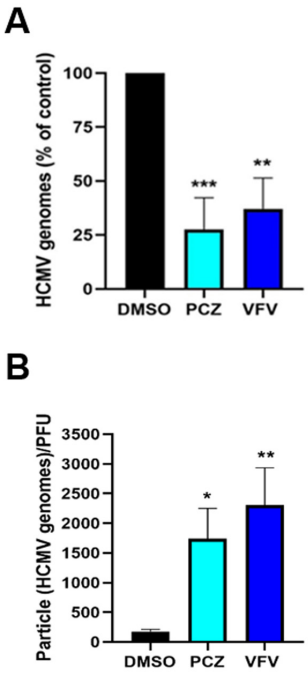

864

865

866

867

868

869

870

871

Figure 6